Break up of the azimuthal symmetry of higher order fiber modes

Israelsen, Stine Møller; Rishøj, Lars Søgaard; Rottwitt, Karsten

Published in:
Optics Express

Link to article, DOI:
10.1364/OE.22.011861

Publication date:
2014

Document Version
Publisher's PDF, also known as Version of record

Break up of the azimuthal symmetry of higher order fiber modes

Stine Møller Israelsen,[1,*] **Lars Søgaard Rishøj,**[1,2] **and Karsten Rottwitt**[1]

[1]*DTU Fotonik, Ørsteds plads byg. 343, 2800 Kgs. Lyngby, Denmark*
[2]*Currently: Boston University, 8 Saint Marys Street, Boston, MA 02215, USA*
[*]*shml@fotonik.dtu.dk*

Abstract: We investigate Bessel-like modes guided in a double cladding fiber where the outer cladding is an aircladding. For very high order LP_{0X}-modes, the azimuthal symmetry is broken and the mode is no longer linearly polarized. This is observed experimentally and confirmed numerically. The effect is investigated numerically using a full vectorial modesolver and is observed to be dependent on the fiber design. The effect on the diffraction free propagation distance of the modes is investigated using a fast Fourier transform propagation routine and compared to the properties of an ideal circularly symmetric mode. The free space properties of modes suffering from break up of azimuthal symmetry are also investigated experimentally by measuring the free space propagation of a LP_{016}-mode excited in the double cladding fiber.

OCIS codes: (060.2400) Fiber properties; (060.4005) Microstructured fibers.

References and links

1. C. D. Poole, J. M. Wiesenfeld, D. J. DiGiovanni, and A. M. Vengsarkar, "Optical fiber-based dispersion compensation using higher order modes near cutoff," J. Lightwave Technol. **12**(10), 1746–1758 (1994).
2. L. Rishøj, Y. Chen, P. Steinvurzel, K. Rottwitt, and S. Ramachandran, "High-energy fiber lasers at non-traditional colours, via intermodal nonlinearities," in *CLEO Technical Digest*, Optical Society of America (2012), p. CTu3M.6.
3. E. Li, X. Wang, and C. Zhang, "Fiber-optic temperature sensor based on interference of selective higher-order modes," Appl. Phys. Lett. **89**(9), 091119 (2006).
4. X. Peng, K. Kim, M. Mielke, T. Booth, J. Nicholson, J. M. Fini, X. Liu, A. DeSantolo, P. S. Westbrook, R. S. Windeler, E. M. Monberg, F. V. DiMarcello, C. Headley, and D. J. DiGiovanni, "Higher-order mode fiber enables high energy chirped-pulse amplification," Opt. Express **21**(26), 32411–32416 (2013).
5. S. Randel, R. Ryf, A. Sierra, P. J. Winzer, A. H. Gnauck, C. A. Bolle, R.-J. Essiambre, D. W. Peckham, A. McCurdy, and R. Lingle, Jr., "6×56-GB/s mode-division multiplexed transmission over 33-km few-mode fiber enabled by 6×6 MIMO equalization," Opt. Express **19**(17), 16697–16707 (2011).
6. J. Durnin, "Exact solutions for nondiffracting beams. I. The scalar theory," J. Opt. Soc. Am. A **4**(4), 651–654 (1987).
7. P. Steinvurzel, K. Tantiwanichapan, M. Goto, and S. Ramachandran, "Fiber-based Bessel beams with controllable diffraction-resistant distance," Opt. Lett. **36**(23), 4671–4673 (2011).
8. S. Ramachandran, J. M. Fini, M. Mermelstein, J. W. Nicholson, S. Ghalmi, and M. F. Yan, "Ultra-large effective area, higher-order mode fibers: a new strategy for high-power lasers," Laser Photon. Rev. **2**(6), 429–448 (2008).
9. P. Steinvurzel, J. Demas, B. Tai, Y. Chen, L. Yan, and S. Ramachandran, "Broadband parametric wavelength conversion at 1 μm with large mode area fibers," Opt. Lett. **39**(4), 743–746 (2014).
10. M. J. Steel, "Reflection symmetry and mode tranversality in microstructured fibers," Opt. Express **12**(8), 1497–1509 (2004).
11. M. J. Steel, T. P. White, C. M. de Sterke, R.C. McPhedran, and L. C. Botten, "Symmetry and degeneracy in microstructured optical fibers," Opt. Lett. **26**(8), 488–490 (2001).

#207866 - $15.00 USD Received 7 Mar 2014; revised 2 May 2014; accepted 2 May 2014; published 9 May 2014

12. J. M. Fini, "Improved symmetry analysis of many-moded microstructure optical fibers," J. Opt. Soc. Am. B **21**(8), 1431–1436 (2004).
13. N. Delen, and B. Hooker, "Free-space beam propagation between arbitrarily oriented planes based on full diffraction theory: a fast Fourier transform approach," J. Opt. Soc. Am. A **15**(4), 857–867 (1998).
14. S. Golowich, "Asymptotic theory of strong spin-orbit coupling in optical fiber," Opt. Lett. **39**(1), 92–95 (2014).

1. Introduction

Higher order modes (HOMs), and in particular Bessel-like modes, have recently attracted much attention within fiber optics. Applications include group velocity dispersion management [1], four wave mixing to access new wavelength regimes [2], sensor applications as for instance temperature sensing [3], chirped pulse amplification in fibers with large effective area [4], and mode division multiplexing for increased capacity in optical communication systems [5]. Bessel beams were first introduced by Durnin *et al.* and possess many interesting properties such as diffraction resistant propagation and selfhealing [6]. Bessel-like beams may be excited in optical fibers, the so-called LP_{0X}-modes, using a UV-induced long period grating (LPG) [7]. These are only approximations to Bessel beams as true Bessel beams require infinite spatial extend and thus are not physically realizable.

The LP_{0X}-modes are an attractive mode group as they have a small sensitivity to mode distortions caused by imperfections in the index profile of the fiber, and they have natural strength to bend distortions. Finally, considering large mode area (LMA) fibers, the mode spacing between the LP_{0X}-modes and the nearest mode group, the LP_{1X}-modes, is an order of magnitude higher than what can be achieved when operating with the conventional LMA fiber for a given effective area. The increased mode spacing suggests significantly less mode coupling, with the mode spacing increasing with the mode order it allows for scaling the fiber to very large effective areas [8]. Recent applications employing the LP_{0X}-modes in LMA fibers include a chirped pulse amplification scheme [4], and high power four wave mixing conducted at 1 μm [9]. We demonstrate break up of the azimuthal symmetry in LP_{0X}-modes, which affects polarization, overlap integrals, mode conversion efficiencies, and free space properties.

Degeneracy and symmetry groups of microstructured fibers have earlier been investigated for low order modes [10–12]. Here, the analysis shows a tendency towards non-degeneracy of the modes [10].

We consider Bessel-like modes excited in a double cladding structure where the outer cladding is an aircladding. The modes are excited with a UV-induced LPG inscribed in the single moded core and propagate in the inner cladding. Such modes have earlier been investigated by e.g. Ramachandran *et al.* [8]. We observe that for very high order Bessel-like modes the azimuthal symmetry is broken and the intensity profile of the mode assumes a bowtie shape, we denote these modes bowtie modes. These modes are investigated experimentally, by considering an LP_{016}-mode generated with minimum 90 % conversion efficiency over a narrow 2 nm bandwidth. We use a new notation to denote the bowtie modes as they are both experimentally and numerically shown to be non linearly polarized. For the bowtie mode corresponding to an LP_{0X}-mode, we use the notation BT_{0X} and thus use the same enumeration of the modes. The first 0 indicates a central lobe and the X denotes the number of rings plus one. The generated mode is hence forward denoted BT_{016}.

In this work, the onset of the investigated bowtie effect and the dependence of this effect on the fiber design are investigated numerically using a full vectorial modesolver, COMSOL. The free space properties of the simulated modes are investigated using a fast Fourier transform propagation tool, designed after the principles described by Delen *et al.* [13]. These properties are compared to those of an ideal mode, with no azimuthal dependence generated with a scalar modesolver.

#207866 - $15.00 USD Received 7 Mar 2014; revised 2 May 2014; accepted 2 May 2014; published 9 May 2014

2. The bowtie effect

To describe the break up of the azimuthal symmetry experimentally, we consider a narrowband LPG inscribed in a double cladding fiber. A microscope image and a sketch of the refractive index profile of the fiber are depicted in Fig. 1.

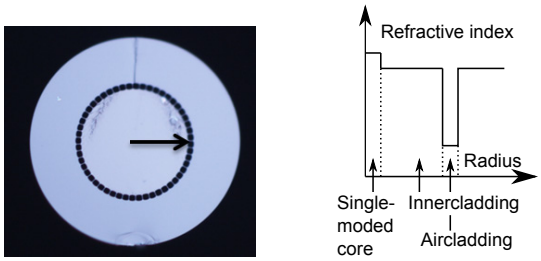

(a) (b)

Fig. 1. (a) Microscope image of the fiber end facet. The outer diameter of the fiber is 156 μm. The radius of the inner cladding is 39 μm and the airholes have a radius of 2 μm. (b) A sketch of the refractive index profile of the fiber along the direction indicated by the arrow in (a).

The conversion efficiency of the LPG, converting from LP_{01} to BT_{016}, is plotted in Fig. 2(a) and an image of the generated mode is depicted in Fig. 2(b), note, the camera is unsaturated. The conversion efficiency shows very little multipath interference indicating excitation of a single mode. From the modal image, it is seen that the mode has a central peak but the azimuthal symmetry is broken compared to an ideal LP_{0X}-mode. We denote this effect the bowtie effect, and thus denote the mode BT_{016}. By slight pertubation of the fiber, the orientation of the bowtie may easily be shifted.

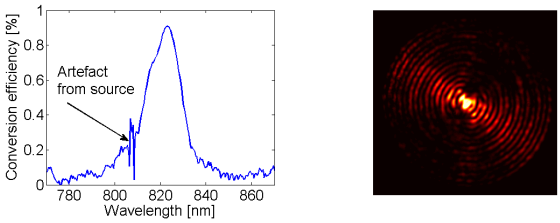

(a) (b)

Fig. 2. (a) Conversion efficiency of the LPG converting LP_{01} to BT_{016} in the aircladding fiber. (b) Image of the BT_{016}-mode after 76 cm of propagation in the aircladding fiber.

To show that the break up of the azimuthal symmetry is neither an imaging nor an interference effect but is in fact a guided mode of the fiber, we use a full vectorial modesolver to find the guided modes in a double cladding structure. The modes are found employing a triangular grid. We consider a double cladding structure with an aircladding as the outer cladding and vary the radius of the holes in the aircladding, but maintain the number of holes in the aircladding to find the onset of the bowtie effect. A sketch of the full simulated fiber geometry and a zoom-in on the aircladding region is depicted in Fig. 3(a) and in Fig. 3(b), respectively. Notice when the radius of the holes in the aircladding is decreased the width of the silica bridges between the airholes is increased. A zoom-in on the mesh in aircladding region is depicted in Fig 3(c), this zoom-in shows the smallest mesh features in the fiber geometry. The size of the smallest features in the fiber geometry, i.e. the airholes, is given and may be compared against

#207866 - $15.00 USD Received 7 Mar 2014; revised 2 May 2014; accepted 2 May 2014; published 9 May 2014

the mesh size.

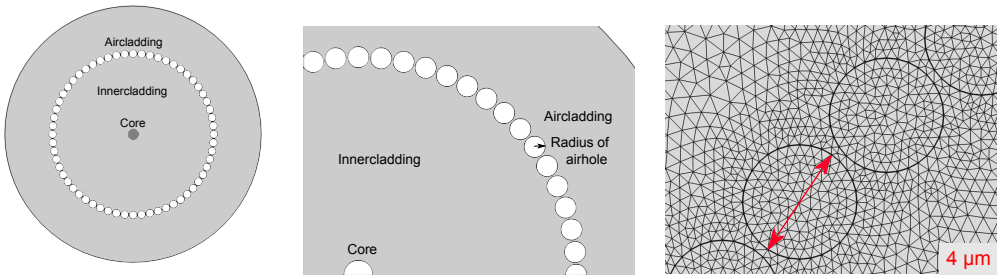

(a) (b) (c)

Fig. 3. (a) Sketch of the simulated fiber geometry. (b) Zoom-in on the airholes in the simulated fiber geometry. (c) Zoom-in on the mesh in the aircladding region where the mesh has the finest structures. The length of the arrow is as indicated in the figure 4 μm.

As the holes become smaller, a smaller amount of field interacts with the holes, and we expect the bowtie effect to be less pronounced. Using the full vectorial modesolver, we find that for mode orders above a certain threshold, the azimuthal symmetry is broken and the mode assumes a bowtie shape. For every mode order, there are two degenerate solutions where the orientations of the bowties are orthogonal. The degeneracy of the solutions allows for every orientation of the bowtie by linear combination. The grid size for the simulation is chosen so that the shape of the mode does not change when choosing a finer resolution. In Fig. 4(a), a simulated modal image of BT_{011} for a hole radius of 2 μm is depicted, the chosen fiber geometry, depicted in Fig. 3(a), is a close approximation to the fiber investigated experimentally. Here the bowtie effect is visible. The normalized variation in the first norm squared of the transverse electric field vector along the first ring in the mode is plotted in Fig. 4(b), along the arrow indicated in Fig. 4(a). We see a sinosoidal variation which is not present for ideal LP_{0X}-modes, the threshold for the onset of the bowtie effect is set to a 25 % variation. Thus it may be concluded that the onset of the bowtie effect for $r = 2$ μm is BT_{011}, whereas for lower hole radii, the threshold is for higher mode orders as the bowtie effect becomes more pronounced with increasing mode order.

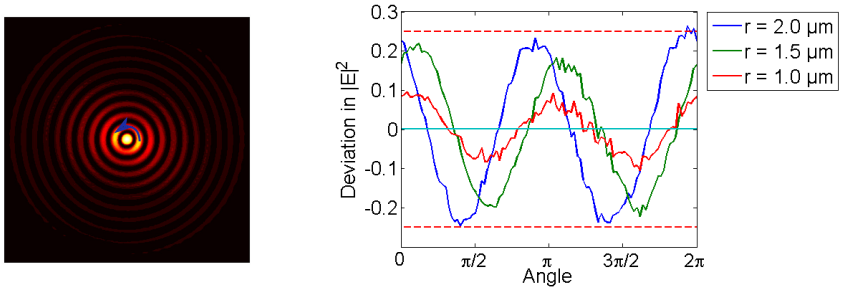

(a) (b)

Fig. 4. (a) BT_{011} in aircladding fiber where the airholes have a radius of 2 μm. The deviation in the first norm square of the transverse electric field vector is to be evaluated along the first ring in the mode. (b) Deviation of the first norm square of the transverse electric field vector along the first ring in BT_{011} guided in the aircladding fiber, the radius of the airholes are varied and the number of holes are conserved.

#207866 - $15.00 USD Received 7 Mar 2014; revised 2 May 2014; accepted 2 May 2014; published 9 May 2014

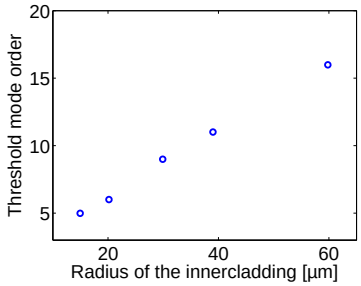

Fig. 5. Onset of the bowtie effect as a function of the radius of the innercladding.

Numerical analysis also shows a large dependence on fiber design such as the radius of the inner cladding, which makes it an important effect to consider in designing optical fiber systems employing HOMs. For smaller radii the bowtie sets in for lower mode order. In Fig 5, the onset of the bowtie effect given by the radial mode order is plotted as function of the radius of the innercladding. The fiber geometry is an aircladding geometry as the one depicted in Fig. 3a. In this analysis, the radius of the airholes and the width of the bridges is maintained, indicating that when reducing the radius of the innercladding the number of holes in the aircladding is reduced. The radius of the airholes and the width of the silica bridges is maintained as a dependency of the airhole radius on the onset of the bowtie effect has just been demonstrated.

Without loss of generality we scale down the studied fiber for better resolution and instead consider a step index fiber with an NA of 0.22 guiding LP_{02} but not LP_{03} to investigate the origin of the bowtie effect and stepwise make the fiber elliptical. With a ellipticity of 0.2, we see an effect similar to the bowtie effect but with two notable differences. The first difference is that in the elliptical fiber, the bowtie is always oriented along the semi-major axis in the ellipse, which does not allow for all orientations of the bowtie, which have been observed experimentally. The second difference is the fact that all solutions for the elliptical fiber are linarly polarized which we in the next section shall demonstrate is not the case for bowtie modes. Ellipticity is thus not the source of the bowtie effect.

We expect that the bowtie effect can be attributed to the fact that the boundary conditions of the radial and the azimuthal component of the electric field are different, thus with increasing field at the boundary as a result of the increasing mode order the effect becomes more dominant and the solutions for the two components differs yielding a resulting bowtie power distribution. It is an effect also expected in an ideal circular fiber as since it is in fact a full vectorial effect. The effect could be an analogue to the effect for hollow core fibers described in a ray picture by Golowich [14].

3. Polarization effects of bowtie modes

As the bowtie effect sets in the polarization of the modes is no longer linear. In Fig. 6(a), the BT_{016}-mode found with the full vectorial modesolver for an aircladding fiber with a hole radius of 2 μm is plotted with arrows indicating the polarization. It is seen that the polarization is orthogonal to the intensity rings in the mode. In the zoom-in on the central rings of the mode in Fig. 6(b), it is seen that there is a π-phaseshift between the polarization of the rings. The tail of the arrow is the point of evaluation. This non linearity of the polarization sets in along with the bowtie effect, the LP_{0X}-modes below the bowtie threshold are approximately linearly polarized. We do not see a gradual transition from the linearly polarized LP_{0X}-mode to the non linear polarization configuration of the bowtie modes depicted in Fig. 6(b). That is a result of

#207866 - $15.00 USD Received 7 Mar 2014; revised 2 May 2014; accepted 2 May 2014; published 9 May 2014

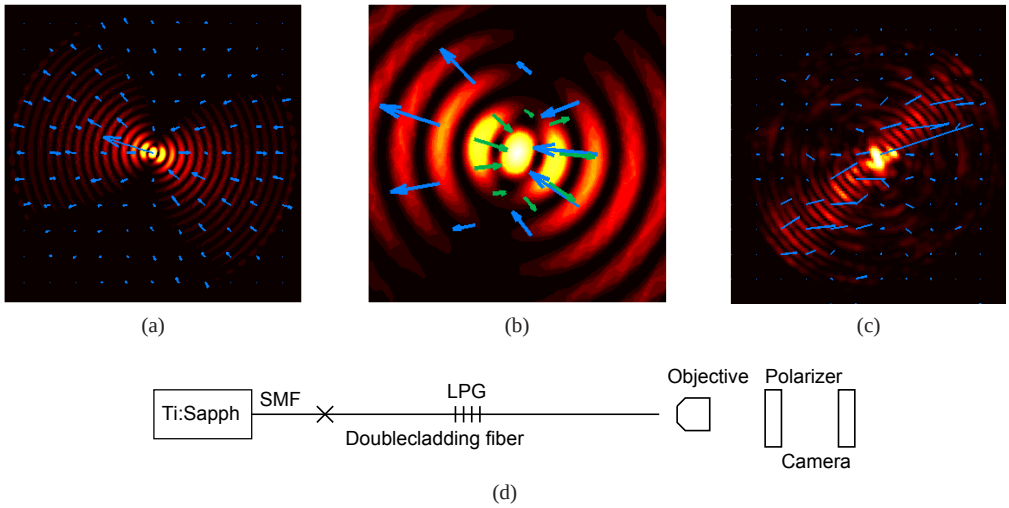

Fig. 6. (a) BT_{016}-mode found with the full vectorial modesolver for an aircladding fiber with a hole radius of 2 μm is plotted with arrows indicating the polarization. (b) Zoom-in on the central rings in the simulated mode. (c) Measured modal image with arrows indicating the polarization of the mode. (d) Setup for measuring the polarization of the mode.

the fact that evaluating the polarization configuration as a function of mode order is a discrete sampling, when instead maintaining the mode order and sweeping the wavelength, a gradual transition from a linearly polarized mode to the characteristic non linearly polarized bowtie mode is found.

In Fig. 6(c), an experimental mapping of the polarization is depicted. The polarization is measured with the setup in Fig. 6(d), the polarizer is turned and for every 10° an image is recorded. Summarizing the intensities for the different angles, it is possible to map the polarization of the mode however, only in an angle of π as the polarizer cannot discriminate a π-phaseshift and the polarization is therefore without arrowheads. It is note, when comparing to the numerical results it is seen that the experimental realization shows the same tendency of a polarization orthogonal to the intensity rings in the mode.

4. Free space properties

To evaluate the performance of the bowtie modes, we compare these modes against ideal LP_{0X}-mode with respect to one of the useful properties associated with Bessel-like modes the diffraction free propagation distance [7].

To find the diffraction free propagation distance experimentally, we perform measurements on the BT_{016}-mode depicted in earlier measurements. We use the setup in Fig. 7(a). The images of the mode upon propagation are stacked and cross sectional lines through the center of the stacked images are plotted in Fig. 7(b). It is speculated, that the airholes in the outer cladding slightly distorts the mode which results in the lack of smoothness in the propagation measurement. In Fig. 7(c), images from the free space propagation are plotted. Note that the bowtie shape is preserved throughout the propagation.

A numerical calculation of the free space properties is performed using a fast Fourier transform propagation method based on the principles of Delen *et al.* [13]. We neglect the contribution from E_z as it is at least 30 dB smaller than the contributions from E_x and E_y. The

#207866 - $15.00 USD Received 7 Mar 2014; revised 2 May 2014; accepted 2 May 2014; published 9 May 2014

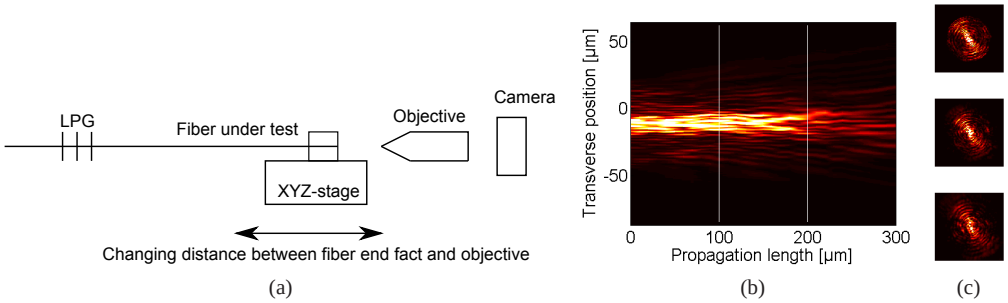

Fig. 7. (a) Setup for measuring the free space propagation of a mode excited by a LPG. (b) Images from the measurements are stacked and plotted along a single axis - the horizontal axis in the mode images in (c). (c) Mode images after, from the top, 0 μm, 100 μm, and 200 μm of free space propagation.

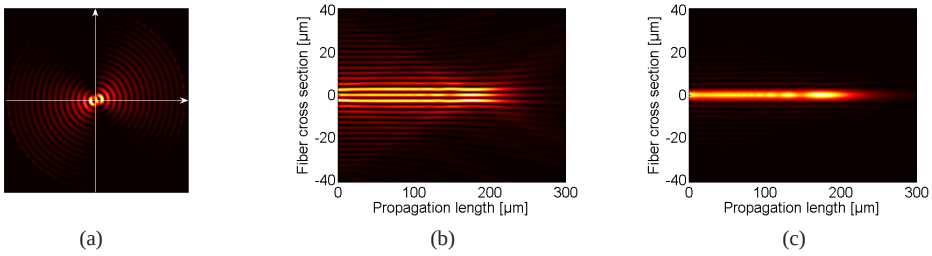

Fig. 8. (a) Modal image of BT_{016} at 823 nm calculated for the aircladding fiber, where the holes have a radius of 2 μm. The axes along which the free propagation is imaged in (b) and (c) are indicated. (b) Free space propagation of BT_{016} along the first axis. (c) Free space propagation of BT_{016} along the second axis.

contributions from E_x and E_y are propagated separately and subsequently added. We perform calculations on BT_{016} at 823 nm found in the aircladding fiber where the holes in the aircladding have a radius of 2 μm. The mode and the propagation along the first and the second axis through the center of the mode are plotted in Fig. 8. The diffraction free propagation distance is defined as the point where the intensity in the center of the beam has dropped to e^{-1} compared to the point of maximum intensity [7]. The BT_{016}-mode has a diffraction free propagation distance of 218 μm as compared to 216 μm for an ideal LP_{0X}-mode found with a scalar mode solver. The bowtie modes shows the same diffraction-resistant behaviour as the Bessel-like modes [7]. When comparing to the experimental measurement, the diffraction free propagation distance is comparable to numerically predicted distance.

The diffraction free propagation distance of LP_{0X}-modes/BT_{0X}-modes (dependent on whether or not the bowtie threshold is reached) guided in the aircladding fiber, where the air-holes have a radius of 2 μm, is plotted as function of mode order and for the modes solved with the scalar modesolver, see Fig. 9. Modes of lower order propagate unstably in any fiber [8], and they are thus not included in the plot. It is observed that the diffraction free propagation distances are much like that of the ideal Bessel-like modes.

#207866 - $15.00 USD Received 7 Mar 2014; revised 2 May 2014; accepted 2 May 2014; published 9 May 2014

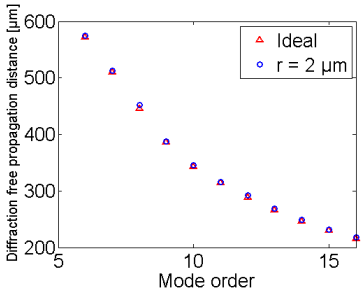

Fig. 9. Diffraction free propagation distance as function of modeorder for LP_{0X}-modes/BT_{0X}-modes in an aircladding fiber and for ideal LP_{0X}-modes found with a scalar mode solver.

5. Conclusion

We have experimentally observed that guiding high order Bessel-like modes in an aircladding structure may lead to a break up of the azimuthal symmetry. This was verified numerically with a full vectorial modesolver, which shows that the break up results in two degenerate modes. We name the break up the bowtie effect after the characteristic shape of the mode. The effect is showed not to originate from an ellipticity of the fiber instead we attribute the effect to different boundary conditions for the azimuthal and the radial component of the electric field. The effect is dependent on the mode order and becomes stronger when going to higher mode orders and is vice versa dependent on the radius of the fiber and lowering the radius results in lowering the onset of the bowtie effect. Once the effect sets in, the mode is no longer linearly polarized but instead orthogonal to the intensity rings in the mode. The free space propagation of the modes are investigated both numerically and experimentally and the both investigations show that the modes may propagate just as far as the ideal Bessel-like modes and that the modes maintain their bowtie shape throughout the propagation.

Acknowledgments

NKT Photonics is acknowledged for manufacturing the fiber. The group of Professor Siddharth Ramachandran at Boston University is acknowledged for facilitating the manufacturing of the LPGs.

#207866 - $15.00 USD Received 7 Mar 2014; revised 2 May 2014; accepted 2 May 2014; published 9 May 2014